P H Y S I C A L   R E V I E W   L E T T E R S

Slowing Down Surface Plasmons on a Moiré Surface

Askin Kocabas, S. Seckin Senlik, and Atilla Aydinli[*]

Department of Physics, Bilkent University, 06800, Ankara, Turkey
(Received 25 April 2008; revised manuscript received 17 December 2008; published 9 February 2009)

We have demonstrated slow propagation of surface plasmons on metallic Moiré surfaces. The phase shift at the node of the Moiré surface localizes the propagating surface plasmons and adjacent nodes form weakly coupled plasmonic cavities. Group velocities around $v_g = 0.44c$ at the center of the coupled cavity band and almost a zero group velocity at the band edges are observed. A tight binding model is used to understand the coupling behavior. Furthermore, the sinusoidally modified amplitude about the node suppresses the radiation losses and reveals a relatively high quality factor ($Q = 103$).

Reducing the group velocity (v_g) of the propagating light in optical materials is an important phenomenon for the basic understanding of light-matter interactions and new technological applications [1,2]. Small group velocities, for instance, can enhance nonlinear processes [3,4] and improve optical conversion efficiencies. Among several approaches, the use of photonic crystals has been the main route to manipulate group velocity. One and two dimensional periodic refractive index modulation can form a photonic crystal which suppresses specific optical modes. Regions of mode suppression are known as photonic band gaps. The characteristics of all modes are defined by dispersion diagrams. Close to the vicinity of the photonic band edges dispersion diagrams flatten and reveal a reduction in group velocity [5]. Furthermore, a line defect photonic crystal also strongly modifies the group velocity in the vicinity of the cutoff wavelength [5–7]. Alternatively, photonic crystal nanocavities can be used as a slow light medium [8]. These approaches do not always allow the desired control on dispersion characteristics corresponding to reduced speed for propagating light. Design of unique dispersion profiles may be possible by the use of coupled resonator optical waveguides cavities (CROWs) [1,9,10].

On the other hand, plasmonic cavities have recently been demonstrated using selective dielectric loading of plasmonic structures [11]. Additionally, Bragg reflectors have been used to observe plasmonic cavities [12] and plasmon hoping along cavities [13]. Previously, propagating surface plasmons with small group velocities have been observed in the vicinity of the band edges of periodic structures [14,15] and in metallic nano particle chains [16]. In this work, we demonstrate plasmonic cavities as well as coupling between the cavities on metallic Moiré surfaces for propagating SPPs with features similar to CROW structures. We show the design, fabrication and the use of these surfaces to obtain propagating SPPs with small group velocities. We show that tight binding description previously applied to CROW structures is suitable for the weakly coupled plasmonic cavities as well.

Figure 1(a) shows the Moiré pattern formed by two superimposed uniform periodic structures having perio-

dicities close to each other [17]. Superimposed periodicities add up to produce nodes and antinodes at the beat frequency of interfering periods and create an additional super periodicity. As seen in Fig. 1(a), the vicinity of the nodes where the amplitude modulation approaches zero forms a cavity. The final Moiré surface profile can be expressed as

$$S(x) = \cos(Gx)\sin(gx), \qquad (1)$$

where $g = \frac{2\pi}{d} = 2\pi\frac{\Lambda_1+\Lambda_2}{2\Lambda_1\Lambda_2}$, $G = \frac{2\pi}{2D} = 2\pi\frac{\Lambda_1-\Lambda_2}{2\Lambda_1\Lambda_2}$, d, D are the uniform periodicity and the periodicity of the super-structure (periodicity of the envelope function), respectively. Λ_1 and Λ_2 are the periodicities of the superimposed uniform gratings. The basic physical principle underlying the cavity behavior of Moiré surface is based on the π phase shift experienced by the SPPs while propagating between the nodes [18]. The cosine term in Eq. (1) acts as an envelope function and modulates the amplitude
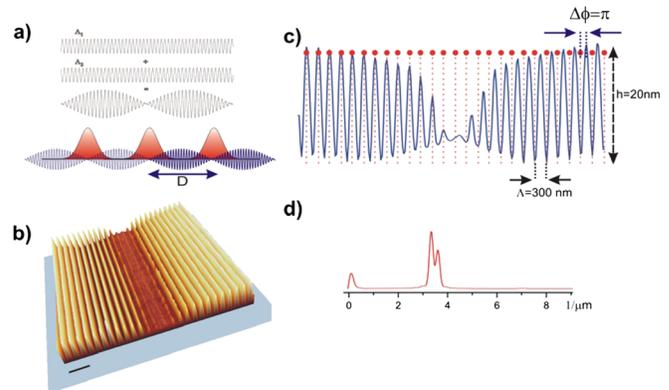
FIG. 1 (color online). (a) Schematic representation of the Moiré surface as a basis of plasmonic coupled cavities. Superimposed two uniform gratings with different periodicities result in a Moiré surface. Red peaks show the localized plasmonic cavity modes. (b) 2D AFM image of a typical Moiré surface (scale bar shows 1 μm). (c) Line profile of AFM image, red dots represents the uniform periodicity and π phase shift occurs at the node of the surface. (d) Power spectrum of the Moiré surface indicating two grating components.

of the grating surface. The envelope function changes sign at the node of the grating and creates a spatial π phase shift. We have fabricated the Moiré patterns using a conventional interference lithography system. Successive exposures at different illumination angles result in a Moiré surface on a photosensitive polymeric surface (AZ 1505). Our interference lithography system allows uniformly exposing an area with a diameter of 3 inches. After a precise calibration of exposure times, large area Moiré surfaces (~ 4 cm^2) were fabricated. Gratings with different periodicities can be fabricated with very high throughput. Furthermore, multiple copies of the preferred gratings can be replicated using soft lithography [11].

Shown in Fig. 1(b) is the AFM image of the fabricated Moiré surface. Surface includes two slightly different periods with periodicities of $\Lambda_1 = 295$ nm and $\Lambda_2 = 305$ nm that result in a superimposed grating. Figure 1(c) indicates the line profile of the AFM image. Red dots represent the uniform periodicity [$\sin(gx)$] of 300 nm. It is clearly seen that at the left side of the pattern red dots coincide with the peaks and while on the right side, red dots coincide with the troughs of the pattern. This indicates the presence of π phase shift located at the node. This phase shift makes Moiré surface act as a distributed Bragg reflector (DBR) with sinusoidally modulated amplitude. Figure 1(d) shows the power spectrum of the line profile clearly indicating the two different harmonic components belonging to the superimposed gratings. In Fig. 1(d), the small difference between the amplitudes of the peaks, results from the difference in exposure times of superimposed grating components. This small difference does

not significantly affect the profile of Moiré surface. These types of Moiré structures have been studied in optical waveguides, diode lasers, fiber based devices and filters with narrow and rectangular-shaped reflection or transmission spectra [18,19].

To study the plasmonic localization and CROW type wave guiding on Moiré surfaces, angle and wavelength dependent reflectivity was measured. In order to construct the band structure, the reflectivity was measured as follows: a spectroscopic ellipsometer (WVASE32) was used to measure the reflection in the visible wavelength range. Kretschmann configuration was used to compensate the momentum mismatch between the incoming light and excited plasmon on Ag-air interface. Plasmonic surfaces were fabricated on a 170 μm thick transparent glass substrate and coated with 50 nm thick Ag film. Sample was then attached onto the prism (Thorlabs, right angle, BK7) using index matching fluids (Nye, OCF-463). Sample was illuminated with a collimated beam with a radius of 1 mm from the prism side and wavelength dependent reflectivity measurements were taken with different incidence angles from which two dimensional reflectivity maps were constructed. In plane wave vector of the SPP depends on the incidence angle and can be tuned by changing the incidence angle between normal incidences of the prism surface and incoming light. Finite set of measurements were interpolated using linear interpolation algorithm with MATLAB.

We note that when surface plasmons at Ag-air interface are excited, angle dependent reflectivity reveals the dispersion characteristics of plasmonic modes. On flat metal
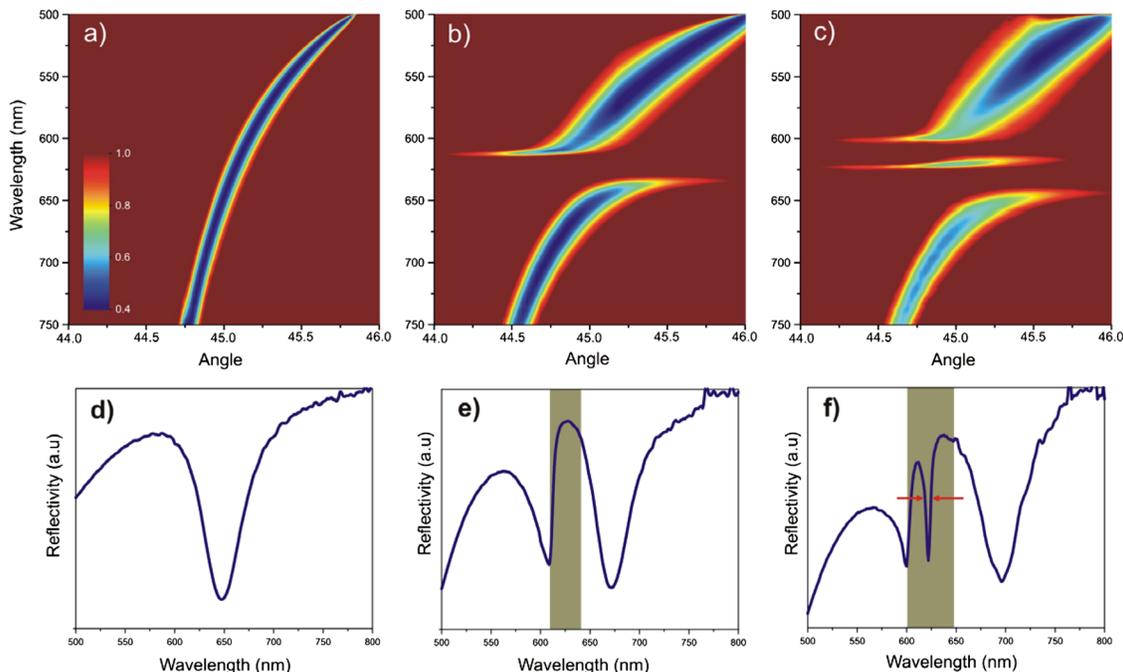
FIG. 2 (color online).   Experimental dispersion curves of SPP's on (a) flat metal surface, (b) uniform grating, (c) Moiré surface, (d), (e),(f) shows the reflectivity of the samples at a constant incidence angle of 45° for each dispersion curve given in (a),(b), (c) respectively. In (e) and (f) highlighted areas indicate the plasmonic band gap region. Color map shows the normalized reflectivity.

surfaces, it is possible to excite SPPs at all wavelengths in the visible range at specific incidence angles. Dispersion on a flat surface asymptotically converges to the surface plasmon resonance frequency of $\omega_p/\sqrt{2}$ where ω_p is the plasma frequency. Figure 2(a) shows experimental reflectivity map of flat metal surfaces indicating the dispersion diagram. It should be noted that reflectivity map shown in Fig. 2 is normalized by the TE reflectivity curve. Effective refractive index of the surface plasmon is highly dispersive in the visible wavelength range. At a given angle, this dispersive behavior restricts the excitation of SPP's in a wide wavelength range. Figure 2(d) shows the wavelength dependent reflectivity at a specific incidence angle. The dip in reflectivity spectrum indicates the SPP excitation. It should be noted that excitation strengths are different for each wavelength due to the dispersion mentioned above.

Periodic metallic structures can scatter the propagating SPPs in the backward direction and form a standing wave. This standing wave formation opens a band gap in the dispersion diagram [20]. In order to observe this, we fabricated a uniform metallic grating structure having a periodicity around 300 nm. Same reflectivity measurements were performed for periodically modulated samples. Reflectivity map in Fig. 2(b) shows a summary of the experimental results. As expected, band gap formation is clearly observed in the dispersion diagram. Dispersion of the band flattens at the vicinity of the band edge. SPP's having a wavelength at band edges create a standing wave localized on the grating structure. Energy difference between the band edges originates from different mode localization profiles, the lower energy configuration corresponding to localization at the peaks of the grating while the higher energy configuration corresponds to localization of the mode on the troughs [20]. As seen in Fig. 2(e), the reflectivity increases inside the SPP excitation region. This reflectivity increase means that SPP excitation in this wavelength range is suppressed due to the band gap. Colored area indicates the band gap region.

To extract the full plasmonic band diagram including the characteristics of the localized mode from the Moiré pattern a further experiment was performed. A nondispersive flat band in the band gap is a key feature of a localized plasmon in a cavity. On the other hand, if individual localized modes start to overlap due to cavity-to-cavity coupling, energies of the corresponding modes split into a new configuration. Furthermore, if these cavities form a periodic structure, linear combination of the individual modes satisfies the Bloch condition and forms a mini dispersive wave-guiding band inside the photonic band gap zone. This phenomenon is called coupled resonator optical wave guiding. This is where the similarity between the Moiré pattern and the CROW structure starts. As described before, the vicinity of the nodes where there is a phase shift of π, acts as a cavity. If the super periodicity is small enough to create a coupling between cavities, a Moiré surface can be modeled as a CROW.

Figure 2(c) shows the dispersion diagram extracted from the reflectivity map of the Moiré surface. The width of the band gap of Moiré surface is relatively larger than that of the uniform grating. This difference is due to the additional grating component in Moiré surface. Second grating component increases the effective grating strength. A weak but clearly noticeable dispersive localized mode appears inside the band gap region. This band indicates the presence of a wave-guiding mode of the coupled plasmonic cavities. This energy band can be modeled by using the tight binding approach, well known in solid state physics and applied to CROW type devices. The simplified expression of the dispersion obtained from the tight binding approximation can be written as [1]

$$\omega(k) = \Omega[1 + \kappa\cos(kD)], \qquad (2)$$

where D, Ω, κ are the super periodicity of the cavities, the resonance frequency of individual cavity and coupling factor, respectively. Upon closer inspection of Fig. 2(c), we find that the dispersion of the localized mode can be fit by the Eq. (2) obtained from the tight binding approximation. Since the coupling coefficient between the cavities can be expressed as $\kappa = \Delta\omega/2\Omega$, $\Delta\omega$ is the CROW band width and resulting in $\kappa \sim 0.006$. The small value of the coupling coefficient displays the weak nature of the coupling between the cavities.

We then study the wavelength dependence of the localized mode in the reflectivity spectrum in Fig. 2(f) and find that the sharp plasmonic excitation has a very small line width of $\Delta\lambda = 6$ nm. The 6 nm line width corresponds to a quality factor of $Q = 103$. This quality factor is relatively high for plasmonic cavities [11–13]. The reason behind this improvement is the suppression of the radiative losses. The overall quality factor can be described as [21]

$$\frac{1}{Q} = \frac{1}{Q_{\mathrm{abs}}} + \frac{1}{Q_{\mathrm{rad}}}, \qquad (3)$$

where Q_{abs} and Q_{rad} are the radiative and absorptive quality factors, respectively. Q_{abs} is dominated by the metallic loss in the plasmonic cavities and Q_{rad} by out-of-plane radiative losses. In general, radiative loss due to leaky modes is caused by scattering of the surface plasmon from higher order grating harmonics and the abrupt change of the localized mode profile in the cavity region [22]. Moiré pattern allows us to get rid of both of these radiative loss sources. As seen in Fig. 1(d), it includes only two harmonic components which can not create significant out-of-plane scattering. Additionally, due to the smooth sinusoidal-like amplitude modulation, the higher wave vector components inside the localized cavity mode are suppressed [22]. To test the loss characteristics of the cavity state we have fabricated four different Moiré surfaces with the super periodicities (D) of 4.5, 7.5, 9, 11.2 μm. The metal thickness of 50 nm and the grating depth of 20 nm were kept the same for each Moiré surface. These parameters are critical for proper excitation of prop-
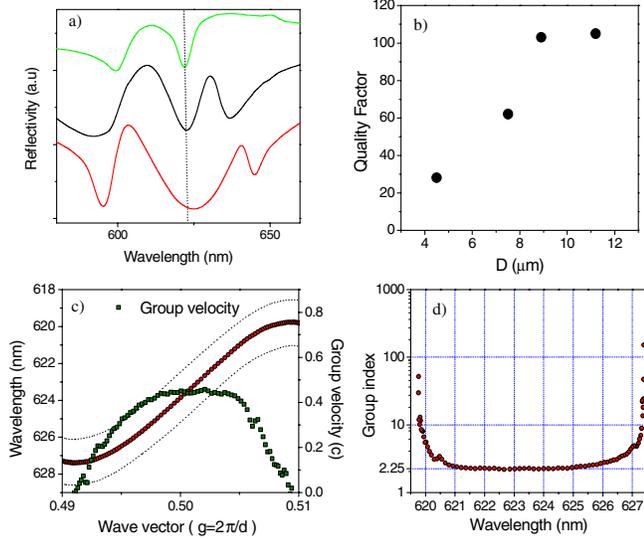
FIG. 3 (color online).   (a) Reflectivity spectra of Moiré surfaces
having different super periodicities ($D = 4.5,\ 7.5,\ 9\ \mu$m).
Dotted line indicates center of the cavity state. (b) Plot of the
quality factors of cavity modes as a function of super periodicity
($D = 4.5, 7.5, 9, 11.2\ \mu$m). (c) Red dots show the experimental
dispersion curve of wave-guiding mode on a Moiré surface
indicating CROW type dispersion and green dots show the
corresponding group velocities. (d) Measured group indices as
a function of wavelength for the CROW type mode.

agating surface plasmons on corrugated metallic surface
using Kretschmann configuration. Figure 3(a) represents
the experimental results. We observed that the resonance
width of the cavity state strongly depends on the periodic-
ity of the super structure. Figure 3(b) shows the corre-
sponding quality factors of the cavity state. It is clear that
the quality factor improves as the super periodicity in-
creases. We observed the optimum quality factor around
103. For larger super periodicities ($>13\ \mu$m), the decreas-
ing number of the cavity inside the illuminated area results
in a decrement in excitation strength. On the other hand,
for shorter super periodicities ($<4\ \mu$m) cavities are
strongly coupled to each other and form a normal propa-
gating surface plasmon band instead of slow propagation.

To analyze the dispersion characteristics of the coupled
cavity wave guiding, we tracked the position of the SPP
excitation wavelength. The measured dispersion diagram
is shown in Fig. 3(c) (red dots). It is seen that dispersion
band gets flattened at the edges of the mini band. In
Fig. 3(c), black dotted lines indicate the -1 dB band width
of the wave-guiding mode. The group velocity can be ex-
pressed as $v_g = d\omega/dk$. The green dots in Fig. 3(c) show
the group velocity throughout the band. The group velocity
is approximately $v_g = 0.44c$ at the center of the band and
approaches to zero in the vicinity of the band edges.

The behavior of the group velocity can also be under-
stood within the framework of the tight binding approach.
Since the dispersion of the band is given by Eq. (2), the
group velocity is [4]

$$v_g(k) = -\Omega D \kappa \sin(kD), \qquad (4)$$

where D, Ω, κ are the superperiodicity of the cavities, the
resonance frequency of individual cavity and coupling
factor, respectively. As seen in Fig. 3(c), group velocity
shows a sinusoidal profile as expected from the tight
binding approximation. The significant factor in the mag-
nitude of group velocity is the coupling coefficient (κ). It is
clear that small values (κ) result in very low group veloc-
ities. Figure 3(d) indicates the corresponding group index
($n_g = c/v_g$) of the SPPs which is nearly constant in the
center of the wave-guiding band and increases dramati-
cally at the band edges.

In conclusion, we have shown that metallic Moiré sur-
faces act as a plasmonic cavity and localize the propagat-
ing surface plasmon due to the π phase shift at its nodes.
Sinusoidally modified amplitude around the cavity region
suppresses the radiation losses and reveals a relatively high
factor ($Q = 103$). Furthermore, weakly coupled cavities
form a low dispersive wave-guiding mode which results in
slowly propagating SPP in band gap region. We have
demonstrated that dispersion characteristics of this mode
can be described by the tight binding model. Small group
velocities and confined behavior of SPPs are promising for
plasmonic nonlinear applications and Moiré surfaces are
good candidates for demonstration of plasmonic lasers.

[1] A. Yariv et al., Opt. Lett. **24**, 711 (1999).
[2] M. Soljacic et al., J. Opt. Soc. Am. B **19**, 2052 (2002).
[3] R. S. Jacobsen et al., Nature (London) **441**, 199 (2006).
[4] T. Kawasaki, D. Mori, and T. Baba, Opt. Express **15**,
10 274 (2007).
[5] Y. A. Vlasov et al., Nature (London) **438**, 65 (2005).
[6] H. Gersen et al., Phys. Rev. Lett. **94**, 073903 (2005).
[7] M. Notomi et al., Phys. Rev. Lett. **87**, 253902 (2001).
[8] T. Tanabe et al., Opt. Express **15**, 7826 (2007).
[9] J. K. S. Poon et al., J. Opt. Soc. Am. B **21**, 1665 (2004).
[10] M. Bayindir, B. Temelkuran, and E. Ozbay, Phys. Rev.
Lett. **84**, 2140 (2000).
[11] A. Kocabas, S. S. Senlik, and A. Aydinli, Phys. Rev. B **77**,
195130 (2008).
[12] J. C. Weeber et al., Nano Lett. **7**, 1352 (2007).
[13] J. C. Weeber et al., Phys. Rev. B **76**, 113405 (2007).
[14] J. G. Rivas et al., Phys. Rev. Lett. **93**, 256804 (2004).
[15] M. Sandtke and L. Kuipers, Nat. Photon. **1**, 573 (2007).
[16] S. A. Maier et al., Nature Mater. **2**, 229 (2003).
[17] J. B. Khurgin, Phys. Rev. A **62**, 013821 (2000).
[18] V. I. Sokolov, in Proc. SPIE (SPIE-International Society
for Optical Engineering, Bellingham, WA, 2001), p. 380.
[19] G. Morthier et al., IEEE Photonics Technol. Lett. **2**, 388
(1990).
[20] W. L. Barnes et al., Phys. Rev. B **54**, 6227 (1996).
[21] Y. Y. Gong and J. Vuckovic, Appl. Phys. Lett. **90**, 033113
(2007).
[22] Y. Akahane et al., Nature (London) **425**, 944 (2003).